Nonlinear Propagation of Dust-Acoustic Waves in An Unmagnetized Collisional Dusty Plasma with Both Nonthermal Electron and Ion Distribution for Damped Korteweg-De Vries Equation

A. Paul[a], G. Mandal[a*], M. R. Amin[a] and P. Chatterjee[b]

[a]*Department of Mathematical and Physical Sciences, East West University, Aftabnagar, Dhaka 1212, Bangladesh.*
[b]*Department of Mathematics, Visva-Bharati, Santiniketan 731235, India.*
[*]Corresponding Author: gdmandal@ewubd.edu

(Received: 5.12.2020 ; Published: 12.3.2021)

Abstract. The nonlinear propagation of dust-acoustic (DA) waves in an unmagnetized dusty and collisional (damped) plasmas (consisting of nonthermal electrons and ions, and mobile negative dust) has been investigated by employing the reductive perturbation technique. It has been found that the presence of dust-ion collisions, the effects of nonthermal electrons and ions, and mobile dust have significantly modified the basic features of nonlinear DA waves. The results of this paper are useful in understanding the basic nonlinear feature of DA wave propagation in laboratory and space dusty electronegative plasmas.

Keywords: Dusty plasma, dust-acoustic (DA) wave, solitary wave, damped forced Korteweg-de Vries equation.

1. INTRODUCTION

Dusty plasmas, which have been observed in earth's magnetosphere, planetary rings, cometary tail, etc [1-3], is a very common field of research in Plasma Physics because of its theoretical features and applications. The presence of dust particles in a plasma introduces different eigen modes, such as, dust acoustic mode (mobile dust), dust ion acoustic mode (immobile dust), dust lattice mode, dust drift mode, etc [4]. Dust acoustic (DA) mode and the existence of this very low-frequency mode was theoretically studied by Rao et al. [5]. In DA mode, the inertia is provided by the mass of dust particles and the restoring force is provided by inertialess electrons and ions [6]. In recent years, many researchers have discussed various aspects of both linear and nonlinear DA wave propagations. In 1996, Mamun et al. studied nonlinear DA wave in an unmagnetized dusty plasma consisting of negatively charged mobile dust particles and Maxwellian (or, Boltzmann) [7] or non-Maxwellian [8] distributed ions. Amin et al. studied nonlinear DA wave in an unmagnetized dusty plasma consisting of mobile charge fluctuating positive dust, trapped electrons and Maxwellian distributed ions [9]. Paul et al. studied nonlinear dynamics of the DA waves in a three component collisionless unmagnetized dusty plasma consisting of nonthermal electrons, trapped ions and mobile negative dust [10].

In all the above-mentioned studies, the authors considered collisionless dusty plasmas, but collisional models in dusty plasmas are present both in natural plasmas (e.g. in laser plasmas, in Earth's ionosphere and in astrophysical plasma environment) and laboratory environments [11-

12]. In a research work, Moslem [13] studied the effects of dust-neutral collision and densities of positive ions and electrons for the propagation of DA wave in a magnetized dusty plasma. He found that due to the collisions in the DA waves, damp waves and the damping rate of the waves depends on the frequency of collisions [13]. Chatterjee et al. studied the analytical solution of the dust ion acoustic (DIA) waves of the damped forced Korteweg-de Vries (KdV) equation in superthermal collisional plasmas [14]. They observed that both the rarefactive and compressive solitary wave solution are possible in this plasma mode. They also observed the effects of different parameters (superthermal parameter, strength and frequency) on the damped forced DIA solitary wave solution through numerical simulation. Many other authors [4, 15-16] also studied collisional models in dusty plasmas and showed the effects of collisional frequency on the wave propagation.

Taking into account the collisional effect of dust in the solution of different dusty plasma modes, in this work, we consider a collisional unmagnetized dusty plasma consisting of nonthermal electrons and ions, and mobile negative dust. We have been particularly interested to observe the effect of the collisional frequency on the DA wave in the dusty plasma.

The paper is organized as follows. The basic governing equations describing the model are stated in Section II. By using the standard reductive perturbation technique [17], the damped KdV equation is derived in Section III. The solution of damped KdV equation is analyzed in terms of different plasma parameters in Section IV. Finally, the conclusion is given in Section V.

II. GOVERNING EQUATIONS

We consider a 1-D, three-component collisional unmagnetized dusty plasma consisting of nonthermal electrons and ions, and mobile negative dust. Here, we consider dust-ion collision.

The nonlinear dynamics of the DA waves in such a collisional dusty plasma system is described by the following set of equations:

$$\frac{\partial n_d}{\partial t} + \frac{\partial}{\partial x}(n_d u_d) = 0 \tag{1}$$

$$\frac{\partial u_d}{\partial t} + u_d \frac{\partial u_d}{\partial x} = \left(\frac{Z_d e}{m_d}\right)\frac{\partial \varphi}{\partial x} - \nu_{id} u_d \tag{2}$$

$$\frac{\partial^2 \varphi}{\partial x^2} = 4\pi e(n_e - n_i + Z_d n_d) \tag{3}$$

where n_s is the number density of the plasma species (e = electron, i = ion and d = dust), u_d is the dust fluid speed, m_d is dust mass, φ is the electrostatic wave potential and ν_{id} is the dust-ion collisional frequency.

For the propagation of the DA wave, we consider both electrons and ions are non-thermal, so we can express n_e and n_i as follows [10]:

$$n_e = n_{e0}\left[1 - \beta\frac{e\varphi}{T_e} + \beta\frac{e^2\varphi^2}{{T_e}^2}\right]e^{e\varphi/T_e} \tag{4}$$

$$n_i = n_{i0}\left[1 + \beta\frac{e\varphi}{T_i} + \beta\frac{e^2\varphi^2}{{T_i}^2}\right]e^{-e\varphi/T_i} \tag{5}$$

where $\beta = 4\alpha/(1+3\alpha)$, α is the nonthermal nature of electrons,T_e and T_i are, respectively, the electron and ion thermal energy.

We consider the normalized variables: $N = n_d/n_{d0}, U = u_d/C_d, \Phi = e\varphi/T_f$ (T_f is the free ion temperature), $X = x/\lambda_D$, $T = t\omega_p$, $\lambda_D = \left(T_f/4\pi Z_d e^2 n_{d0}\right)^{1/2}$, $C_d = \left(Z_d T_f/m_d\right)^{1/2}$ and $\omega_p = \left(4\pi {Z_d}^2 e^2 n_{d0}/m_d\right)^{1/2}$. The normalized form of Eq. (1) - (3) are given below:

$$\frac{\partial N}{\partial T} + \frac{\partial}{\partial X}(NU) = 0 \tag{6}$$

$$\frac{\partial U}{\partial T} + U\frac{\partial U}{\partial X} = \left(\frac{Z_d T_f}{m_d {C_d}^2}\right)\frac{\partial \Phi}{\partial X} - \upsilon U \tag{7}$$

$$\frac{\partial^2 \Phi}{\partial X^2} = \mu_e e^{\sigma_e \Phi}(1 - \beta\sigma_e\Phi + \beta{\sigma_e}^2\Phi^2) - \mu_i e^{-\sigma_e \Phi}(1 + \beta\sigma_i\Phi + \beta{\sigma_i}^2\Phi^2) + N \tag{8}$$

where $\sigma_e = T_f/T_e, \sigma_i = T_f/T_i, \mu_e = n_{e0}/Z_d n_{d0}, \mu_i = n_{i0}/Z_d n_{d0}$ and $\nu = \nu_{id}/\omega_p$.

III. DERIVATION OF THE DAMPED KdV EQUATION

To derive the modified KdV equation, we employ the reductive perturbation technique [17]. We introduce the stretched coordinates [18-19]:

$$\xi = \epsilon^{1/2}\left(X - V_p T\right) \tag{9}$$

and

$$\tau = \epsilon^{3/2} T \tag{10}$$

where ϵ is a smallness parameter $(0 < \epsilon < 1)$ that measures the weakness of the dispersion, and V_p is the nonlinear wave phase velocity normalized by C_d. Now we expand the variables N, U, Φ and ν in the power series of ϵ:

$$N = 1 + \epsilon N^{(1)} + \epsilon^2 N^{(2)} + \ ... \tag{11}$$

$$U = \epsilon U^{(1)} + \epsilon^2 U^{(2)} + \ ... \tag{12}$$

$$\Phi = \epsilon \Phi^{(1)} + \epsilon^2 \Phi^{(2)} + \ ... \tag{13}$$

$$\upsilon = \epsilon^{3/2} \nu_{id0} \tag{14}$$

Now substituting these expressions in equations (6)-(8), we get equations of different powers of ϵ. Solving for $N^{(1)}$, $U^{(1)}$ and V_p, we get the following sets of relations:

$$N^{(1)} = P\Phi^{(1)} \tag{15}$$

$$U^{(1)} = PV_p\Phi^{(1)} \tag{16}$$

$$V_p = \sqrt{-\frac{Q}{P}} \tag{17}$$

where $P = (\beta - 1)(\mu_e\sigma_e + \mu_i\sigma_i)$ and $Q = Z_d T_f/m_d {C_d}^2$.

Again, using equations (11)-(17), we obtain equations containing $N^{(2)}$ and $U^{(2)}$ from normalized equations (6)-(8) as follows:

$$\frac{\partial^2 \Phi^{(1)}}{\partial \xi^2} = -P\Phi^{(2)} + R\left[\Phi^{(1)}\right]^2 + N^{(2)} \tag{18}$$

$$\frac{\partial N^{(1)}}{\partial \tau} - V_p \frac{\partial N^{(2)}}{\partial \xi} + \frac{\partial U^{(2)}}{\partial \xi} + \frac{\partial N^{(1)} U^{(1)}}{\partial \xi} = 0 \tag{19}$$

$$\frac{\partial U^{(1)}}{\partial \tau} - V_p \frac{\partial U^{(2)}}{\partial \xi} + U^{(1)} \frac{\partial U^{(1)}}{\partial \xi} = Q \frac{\partial \Phi^{(2)}}{\partial \xi} - \nu_{id0} U^{(1)} \tag{20}$$

where $R = (\mu_e {\sigma_e}^2 - \mu_i {\sigma_i}^2)/2$.

Now differentiating equation (18) with respect to ξ and using equations (19)-(20), we can obtain the damped KdV equation.

$$\frac{\partial \Phi^{(1)}}{\partial \tau} + A\Phi^{(1)} \frac{\partial \Phi^{(1)}}{\partial \xi} + B \frac{\partial^3 \Phi^{(1)}}{\partial \xi^3} + C\Phi^{(1)} = 0 \tag{21}$$

where $A = Y/X, B = 1/X, C = Z/X$ and $X = P^2 V_p/Q - PV_p, Y = P^3 V_p/Q - 2P^2 - 2R$, $Z = P^2 V_p \nu_{id0}/Q$.

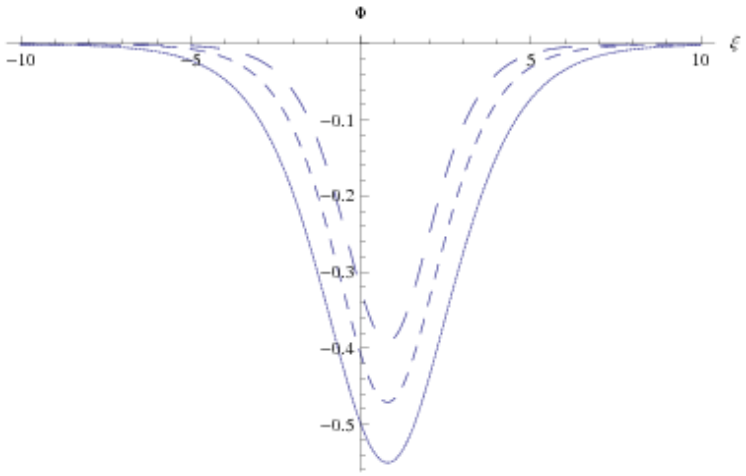

FIGURE 1. The variation of the solution, Φ, of the damped KdV equation as a function of the position coordinate ξ for three values of non-thermal parameter β. In solid curve $\beta = 0.6$, in dashed curve $\beta = 0.4$ and in long-dashed curve $\beta = 0.2$. The values of the other parameters are the following: $M_0 = 0.4$, $\tau = 2$, $n_{e0} = 4 \times 10^4\ cm^{-3}$, $n_{i0} = 7 \times 10^4\ cm^{-3}$, $n_{d0} = 10^4 - 4 \times 10^4\ cm^{-3}$, $T_f = 4 \times 10^{-13}\ erg$, $T_e = 1.3 \times 10^{-11}\ erg$ and $T_i = 4.8 \times 10^{-13}\ erg$.

IV. SOLUTION OF THE DAMPED KdV EQUATION

Collision changes the standard KdV equation into damped KdV equation and that significantly modifies the behavior of nonlinear waves.

In the absence of C, equation (21) becomes the well-known KdV equation

$$\frac{\partial \Phi^{(1)}}{\partial \tau} + A\Phi^{(1)} \frac{\partial \Phi^{(1)}}{\partial \xi} + B \frac{\partial^3 \Phi^{(1)}}{\partial \xi^3} = 0 \tag{22}$$

and the solitary wave solution of the KdV equation is

$$\Phi^{(1)} = \Phi_m \mathrm{sech}^2 \left(\frac{\xi - M\tau}{W} \right) \tag{23}$$

where $\Phi_m = 3M/A$ and $W = 2\sqrt{B/M}$ (M is the Mach Number). In this case,

$$I = \int_{-\infty}^{\infty} \left[\Phi^{(1)}\right]^2 d\xi \tag{24}$$

is a conserved quantitv.

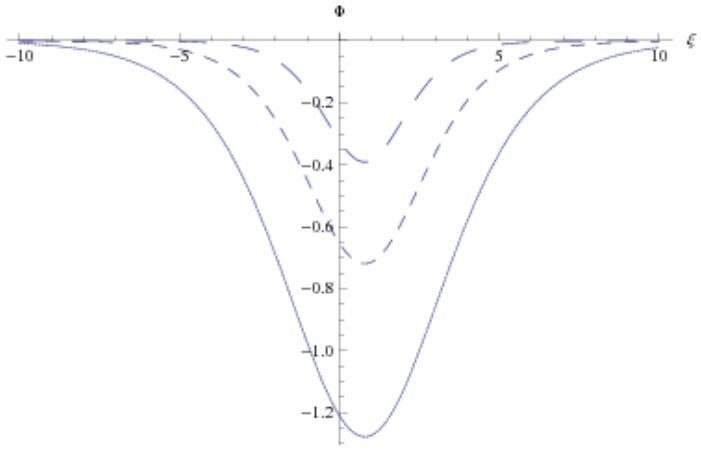

FIGURE 2. The variation of the solution, Φ, of the damped KdV equation as a function of the position coordinate ξ for $n_{d0} = 4 \times 10^4\ cm^{-3}$ (solid curve), $n_{d0} = 2 \times 10^4\ cm^{-3}$ (dashed curve) and $n_{d0} = 10^4\ cm^{-3}$ (long-dashed curve). The values of the other parameters are the following: $\beta = 0.2.2$, $M_0 = 0.4$, $\tau = 2$, $n_{e0} = 4 \times 10^4\ cm^{-3}$, $n_{i0} = 7 \times 10^4\ cm^{-3}$, $T_f = 4 \times 10^{-13}\ erg$, $T_e = 1.3 \times 10^{-11}\ erg$ and $T_i = 4.8 \times 10^{-13}\ erg$.

For small values of C (i.e., in presence of damping), we consider the solution (23) has the form

$$\Phi^{(1)} = \Phi_m(\tau)\text{sech}^2\left(\frac{\xi - M(\tau)\tau}{W(\tau)}\right) \tag{25}$$

where $\Phi_m(\tau) = 3M(\tau)/A$, $W(\tau) = 2\sqrt{B/M(\tau)}$ and $M(\tau)$ is an unknown function of τ . Now differentiating I, i.e. equation (24), with respect to τ and using equation (21) we get

$$\frac{dI}{d\tau} + 2CI = 0 \tag{26}$$

Solving the ordinary differential equation by considering the initial conditions $I = I_0$ when $\tau = \tau_0$, we get

$$I = I_0 exp[-2C(\tau - \tau_0)] \tag{27}$$

Substituting equation (25) into equation (24), we get

$$\begin{aligned} I(\tau) &= \int_{-\infty}^{\infty} {\Phi_m}^2(\tau)\text{sech}^4\left(\frac{\xi - M(\tau)\tau}{W(\tau)}\right) d\xi \\ &= \frac{4}{3}[\Phi_m(\tau_0)]^2 W(\tau_0) exp[-2C(\tau - \tau_0)] \end{aligned} \tag{28}$$

where $\Phi_m(\tau_0) = 3M(\tau_0)/A$ and $W(\tau_0) = 2\sqrt{4B/M(\tau_0)}$.

The value of $M(\tau)$ is obtained by

$$M(\tau) = M(\tau_0)exp\left[-\frac{4}{3}C(\tau-\tau_0)\right]. \quad (29)$$

Therefore, equation (25) is the analytical solution of the damped KdV equation.

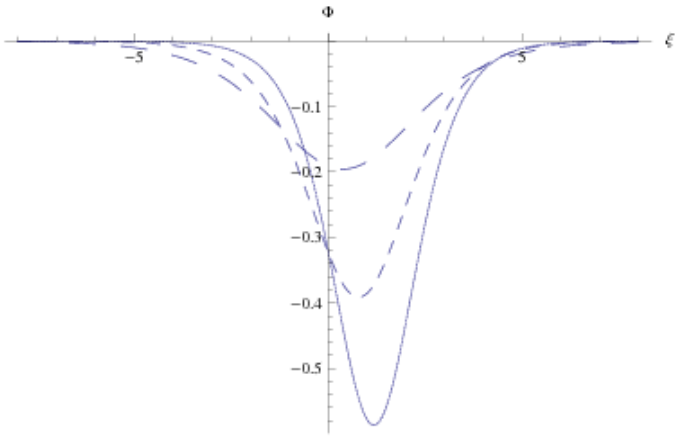

FIGURE 3. The variation of the solution Φ, , of the damped KdV equation as a function of the position coordinate ξ for different values oM_0f M_0. The solid curve is for $M_0 = 0.6$, whereas dashed curve and the long-dashed curve are for $M_0 = 0.4$ and $M_0 = 0.2$, respectively. The values of the other parameters are the following: $\beta = 0.2$, $\tau = 2$, $n_{e0} = 4 \times 10^4\, cm^{-3}$, $n_{i0} = 7 \times 10^4\, cm^{-3}$, $n_{d0} = 4 \times 10^4\, cm^{-3}$, $T_f = 4 \times 10^{-13}\, erg$, $T_e = 1.3 \times 10^{-11}\, erg$ and $T_i = 4.8 \times 10^{-13}\, erg$.

V. EFFECTS OF IMPORTANT PARAMETERS

In this section, we study the effects of the slow variables ξ and time τ on the potential Φ and the amplitude Φ_m of the DA wave. In addition, we study the effects of some important plasma parameters, such as non-thermal parameter β, damping parameter ν_{id0} and density of dust particles n_{id0}, on the wave potential Φ, wave amplitude Φ_m and width W. In the figures we show the results of our study, where we set the values of the following parameters: $e = 4.8 \times 10^{-10}$ CGS unit, $0 < \beta < 1$, $\nu_{id0} = 0.01 - 0.1$, $n_{e0} = 4 \times 10^4\, cm^{-3}$, $n_{i0} = 7 \times 10^4\, cm^{-3}$, $n_{d0} = 10^4 - 4 \times 10^4\, cm^{-3}$, $m_d = 10^{-10}\, gm$, $Z_d = 3 \times 10^3$, $T_f = 4 \times 10^{-13} erg$, $T_e = 1.3 \times 10^{-11} erg$ and $T_i = 4.8 \times 10^{-13} erg$.

Figure 1 shows the variation of the electrostatic potential Φ, of the damped KdV equation as a function of the position coordinate ξ for different values of non-thermal parameter β. In the figure, the solid curve, dashed curve and long-dashed curve are for $\beta = 0.6$, $\beta = 0.4$ and $\beta = 0.2$, respectively. Figure 2 shows the same for three different values of n_{d0}: $n_{d0} = 4 \times 10^4\, cm^{-3}$ (solid curve), $n_{d0} = 2 \times 10^4\, cm^{-3}$ (dashed curve) and $n_{d0} = 10^4\, cm^{-3}$ (long-dashed curve). Both figures show that the solitary wave has a negative potential and the potential function decreases with the increment of β (in Fig. 1) and n_{d0} (in Fig. 2).

Figure 3 and Figure 4 also show the variation of the electrostatic potential Φ, of the damped KdV equation as a function of the position coordinate ξ for different values of M_0 (in Fig. 3) and ν_{id0} (in Fig. 4). In Figure 3, $M_0 = 0.6$ (solid curve), $M_0 = 0.4$ (dashed curve) and $M_0 = 0.2$ (long-dashed curve). On the other hand, in Figure 4, $\nu_{id0} = 0.01$ (solid curve), $\nu_{id0} = 0.21$ (dashed

curve) and $\nu_{id0} = 0.41$ (long-dashed curve). In Figure 3 the amplitude of the negative potential increases with the increment of the parameter M_0. But in Figure 4, the amplitude of the potential decreases with the increment of the parameter ν_{id0}. In both cases, the bottom of the dip shaped solitary wave changes its position along ξ −axis for the variation of parameter. The bottom moves to the right for higher values of M_0 (in Fig. 3) and that for lower values of ν_{id0} (in Fig. 4).

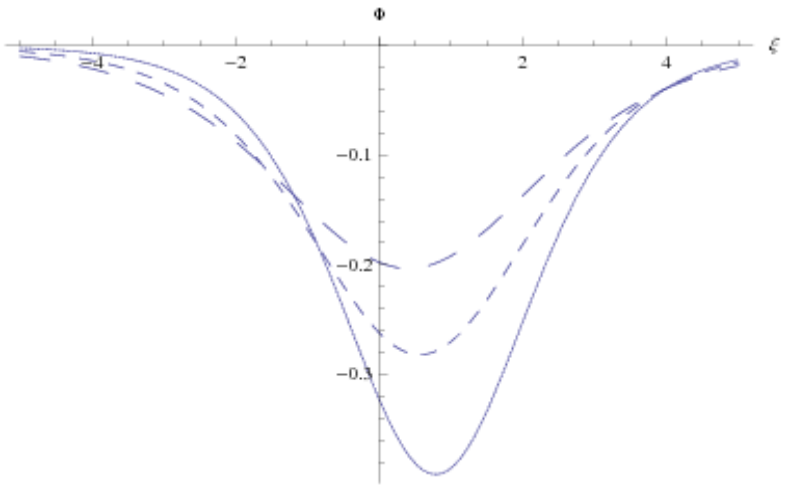

FIGURE 4. The variation of the solution, Φ, of the damped KdV equation as a function of the position coordinate ξ for the variation of the damping parameter ν_{id0}. The solid curve is for $\nu_{id0} = 0.01$, dashed curve is for $\nu_{id0} = 0.21$ and the long-dashed curve is for $\nu_{id0} = 0.41$. The values of the other parameters are the following: $\beta = 0.2$, $\tau = 2$, $n_{e0} = 4 \times 10^4\, cm^{-3}$, $n_{i0} = 7 \times 10^4\, cm^{-3}$, $n_{d0} = 4 \times 10^4\, cm^{-3}$, $\mathrm{T_f} = 4 \times 10^{-13}$ erg, , $T_e = 1.3 \times 10^{-11}\, erg$ and $T_i = 4.8 \times 10^{-13}\, erg$.

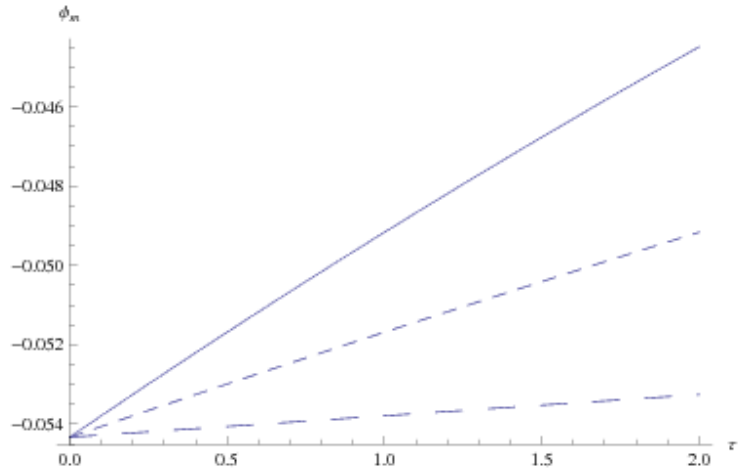

FIGURE 5. The variation of the amplitude, Φ_m, of the solitary wave as a function of time, τ , for different values of ν_{id0}. The solid curve is for $\nu_{id0} = 0.1$, whereas the dotted curve and the long-dashed curve are for $\nu_{id0} = 0.05$ and $\nu_{id0} = 0.01$, respectively. The values of the other parameters are the following: $\beta = 0.2$, $M_0 = 0.1$, $n_{e0} = 4 \times 10^4\, cm^{-3}$, $n_{i0} = 7 \times 10^4\, cm^{-3}$, $n_{d0} = 4 \times 10^4\, cm^{-3}$, $T_f = 4 \times 10^{-13}\, erg$, $T_e = 1.3 \times 10^{-11}\, erg$ and $T_i = 4.8 \times 10^{-13}\, erg$.

Amplitude, Φ_m, of the solitary wave verses time, τ, is drawn in Figure 5. In the figure the solid curve, dotted curve and long-dashed curve are for $\nu_{id0} = 0.1$, $\nu_{id0} = 0.05$ and $\nu_{id0} = 0.01$,

respectively. Figure 5 shows that the amplitude of the wave increases with the increment of time and damping parameter ν_{id0}.

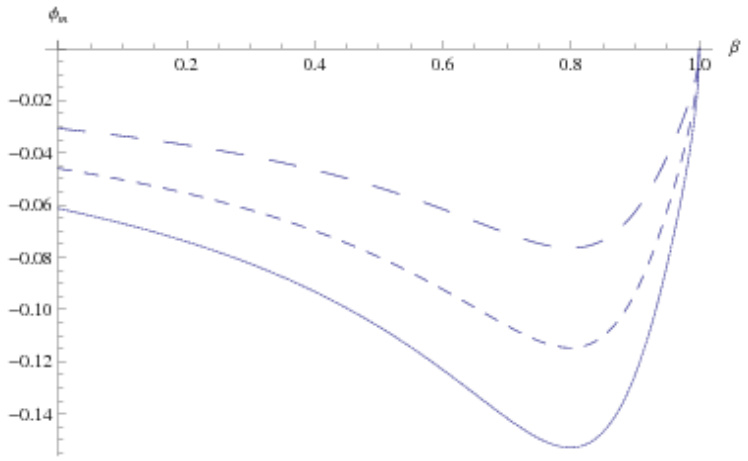

FIGURE 6. The variation of the amplitude, Φ_m, of the solitary wave as a function of β for different values of M_0. The solid curve, dotted curve and the long-dashed curve are for $M_0 = 0.2$, $M_0 = 0.15$ and $M_0 = 0.1$, respectively. The values of the other parameters are the following: $\beta = 0.2$, $\nu_{id0} = 0.01$, $\tau = 2$, $n_{e0} = 4 \times 10^4\ cm^{-3}$, $n_{i0} = 7 \times 10^4\ cm^{-3}$, $n_{d0} = 4 \times 10^4\ cm^{-3}$, $T_f = 4 \times 10^{-13}\ erg$, $T_e = 1.3 \times 10^{-11}\ erg$ and $T_i = 4.8 \times 10^{-13}\ erg$.

Figure 6 shows a graph of the amplitude, Φ_m, of the solitary wave as a function of the nonthermal parameter β for different values of M_0. In the figure $M_0 = 0.2$, $M_0 = 0.15$ and $M_0 = 0.1$ are for solid curve, dotted curve and long-dashed curve, respectively. We observe that the amplitude decreases with β up to a certain value, but after that value of β (approximately 0.8 in this case) amplitude of the wave increases with β. We also observe that a smaller value of M_0 gives a higher amplitude.

Figure 7 shows the variation of the width of the solitary wave as a function of time τ for three different values of ν_{id0}. In the figure the solid curve is for $\nu_{id0} = 0.3$, the dotted curve is for $\nu_{id0} = 0.2$ and long-dashed curve is for $\nu_{id0} = 0.1$. Figure 7 shows that the width of the solitary wave increases with both time and ν_{id0}.

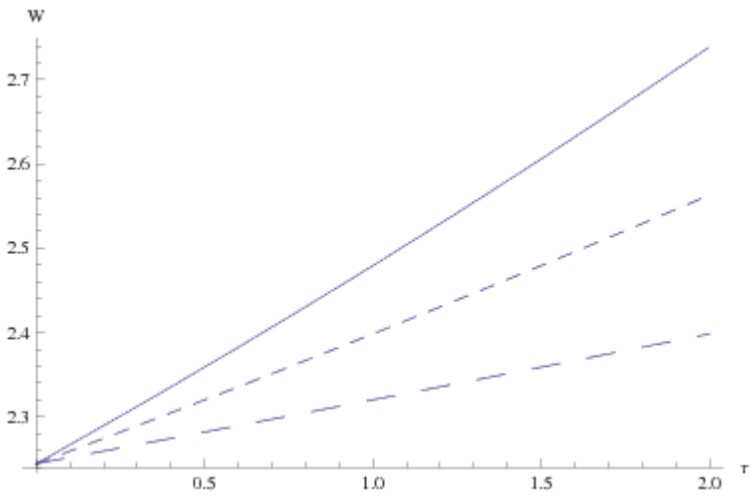

FIGURE 7. The variation of the width, W of the solitary wave as a function of the time τ for different values of ν_{id0}. The solid curve is for $\nu_{id0} = 0.3$, whereas dotted curve and the long dashed curve are for $\nu_{id0} = 0.2$ and $\nu_{id0} = 0.1$, respectively. The values of the other parameters are the following: $\beta = 0.2$, $M_0 = 0.4$, $n_{e0} = 4 \times 10^4\ cm^{-3}$, $n_{i0} = 7 \times 10^4\ cm^{-3}$, $n_{d0} = 4 \times 10^4\ cm^{-3}$, $T_f = 4 \times 10^{-13}\ erg$, $T_e = 1.3 \times 10^{-11}\ erg$ and $T_i = 4.8 \times 10^{-13}\ erg$.

VI. CONCLUSION

In this paper, we have studied the nonlinear propagation of DA solitary waves in an unmagnetized dusty plasma consisting of mobile negative dust, nonthermal electrons and ions in presence of dust-ion collision. The propagation of the amplitude of the nonlinear DA waves in electronegative dusty plasma is considered by analyzing the solution of KdV equation and this equation is derived by using reductive perturbation technique. By varying different plasma parameters the detailed numerical analysis of wave potential, amplitude and width of the DA wave is performed.

The results which have been found in this investigation are as follows:

1. It is found that by increasing the parameter β and n_{d0} the potential of the solitary wave is sharply decreased.
2. The bottom of the solitary wave with negative potential moves its position (to the right or left) for different values of M_0 and ν_{id0}.
3. The parameters τ, β and M_0 have significant effects on the amplitude of the solitary wave.
4. We found that the amplitude and the width of the solitary wave varies with the variation of damping parameter ν_{id0}.

Here we have shown how the basic features of the nonlinear DA solitary waves in a collisional plasma are modified by the presence of nonthermal electrons and ions, and mobile negatively charged dust grains in it.

REFERENCES

1. C. K. Geortz : Rev. Geophys. **27**, 217 (1989).
2. P. K. Shukla and A. A. Mamun: Introduction to Dusty Plasma Physics. IOP, London (2002) and references therein.
3. O. Havens, F. Melandso, C. L. Hoz, T. K. Aslaksen and T. Hartquist: Phys. Scr. **45**, 433 (1992).
4. T. K. Das, S. Choudhury, A. Saha and P. Chatterjee: J. Fizik Malaysia **38(1)**, 010016 (2017).
5. N. N. Rao, P. K. Shukla, and M. Y. Yu, Planet. Space Sci.0032-0633 **38**, 543 (1990).
6. A. A. Mamum, J. Plasma Phys. **59**, 575 (1998).
7. A. A. Mamum, R. A. Cairns, and P. K. Shukla, Phys. Plasmas **3**, 702 (1996a).
8. A. A. Mamum, R. A. Cairns, and P. K. Shukla, Phys. Plasmas **3**, 2610 (1996b).
9. M. R. Amin, S. K. Paul, G. Mandal, and A. A. Mamum, J. Plasmas Phys. **76**(parts 3-4), 477 (2010).
10. A. Paul, G. Mandal, A. A. Mamun, *and* M. R. Amin, Physics of Plasmas **20**, 104505 (2013).
11. A. V. Volosevich and C. V. Meister, Contrib. Plasma Phys. **42**, 61 (2002).
12. T. K. Das, A. Saha, N. Pal and P Chatterjee, Physics of Plasmas **24**, 073707 (2017).
13. M. Shalaby, S. K. El-Labany, E. F. El-Shamy, and M. A. Khaled, Astrophys. Space Sci. **326**, 273 (2010).
14. P. Chatterjee and R. Ali, Z. Naturfosch A **73(2)**, 0385 (2017).
15. M. Shalaby, S. K. El-Labany, E. F. El-Shamy, and M. A. Khaled, Astrophys. Space Sci. **326**, 273 (2010).
16. R. L. Merlino, IEEE Trans. Plasma Sci. **25**, 60 (1997).
17. H. Washimi and T. Sarma, Phys. Rev. Lett. **17**, 996 (1966).
18. H. Schamel, J. Plasma Phys. **14**, 905 (1972).
19. H. Schamel, J. Plasma Phys. **9**, 377 (1973).